

Dielectric Boundary Smoothing in Finite Difference Solutions of the Poisson Equation: An Approach to Improve Accuracy and Convergence

Malcolm E. Davis* and J. Andrew McCammon

Department of Chemistry, University of Houston, Houston, Texas 77204-5641

Received 19 December 1990; accepted 1 April 1991

Finite difference methods are becoming very popular for calculating electrostatic fields around molecules. Due to the large amount of computer memory required, grid spacings cannot be made extremely small in relation to the size of the van der Waals radii of the atoms. As a result, the calculations make a rather crude approximation to the molecular surface by defining grid line midpoints discontinuously as either interior or exterior. We present a method which "smoothes" the boundary, but more accurately models the potential from the analytic solution of the discontinuous dielectric problem and improves convergence in electrostatic energy calculations. In addition, a small improvement in convergence rate is observed.

INTRODUCTION

Finite difference solutions for electrostatic potentials provide for fast, relatively accurate means for calculating electrostatic interaction energies and forces and have become widely used.¹⁻⁸ These techniques have demonstrated utility in Brownian dynamic simulations, as well as in binding energy, conformational energy, and pK_a shift calculations.^{9,10}

The details of the molecular surface have been found to be of special functional importance for proteins. Surface topology and electrostatic complementarity have been indicated as playing important roles in protein-substrate binding.¹¹ Similarly, Brownian dynamics studies have indicated the importance of the electrostatic "focusing" produced by clefts and pockets on protein surfaces.^{7,12}

In light of this significance, one persistent area of concern has been the deviation of the calculated finite difference potentials from corresponding analytic solutions near dielectric boundaries, in systems where analytic solutions are available for comparison. These deviations result in part from the crude mapping of the surface produced by current methods for assigning dielectric coefficient values at the grid-line midpoints. While charges have long been split over the neighboring grid points¹³ to allow a smooth variation as a charge was translated relative to the grid, dielectric points have been assigned either interior or exterior values, which results in a squared-off representation of the molecule. In this

article, we will demonstrate that smoothing the dielectric boundary when assigning values actually produces potentials that more accurately match the analytic solutions of the corresponding discontinuous dielectric problem. In addition, the smoothly varying dielectrics slightly improve the rate of convergence of the numerical solution.

THEORY

The electrostatic potential satisfies the differential form of Gauss's law

$$-\nabla \cdot \epsilon(\mathbf{r}) \nabla \phi(\mathbf{r}) = \rho(\mathbf{r}) \quad (1)$$

Calculating the electrostatic potential in an infinite parallel plate capacitor with two different dielectrics, as shown in Figure 1(a), is a standard introductory electrostatics problem. In each of the regions, ϵ is constant and the general solution to the differential equation is $\phi = Ax + B$. Applying the boundary conditions at $x = 0$, $x = 1 + a$, and $x = 3$, one obtains the solution.

$$\phi(x) = \begin{cases} \frac{\epsilon_r(\phi_3 - \phi_0)}{(\epsilon_r + 2\epsilon_l) + a(\epsilon_r - \epsilon_l)} x + \phi_0 & r < 1 + a \\ \frac{\epsilon_l(\phi_3 - \phi_0)}{(\epsilon_r + 2\epsilon_l) + a(\epsilon_r - \epsilon_l)} x \\ + \frac{(\epsilon_r - \epsilon_l)(1 + a)\phi_3 + 3\epsilon_l\phi_0}{(\epsilon_r + 2\epsilon_l) + a(\epsilon_r - \epsilon_l)} & r > 1 + a \end{cases} \quad (2)$$

for the continuum representation of the problem.

*Author to whom all correspondence should be addressed.

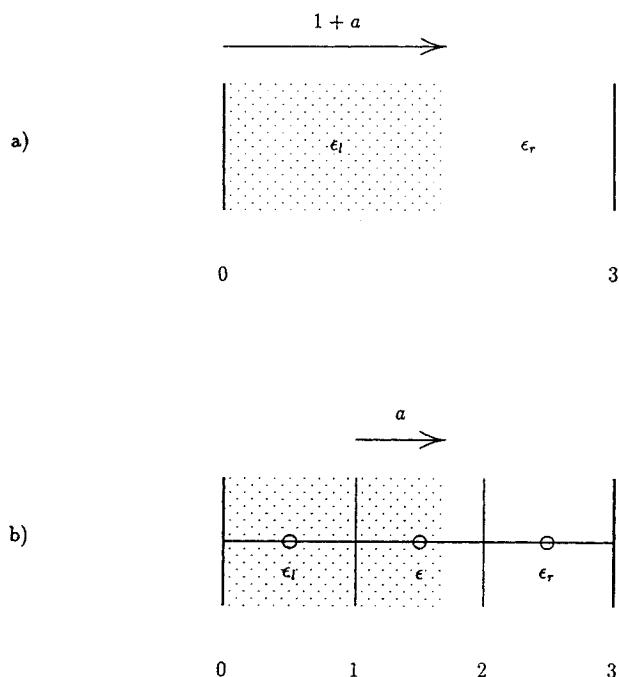


Figure 1. The geometry of a parallel plate capacitor with two different dielectric slabs viewed from a continuum (a) and a finite difference (b) viewpoint.

The finite difference form of eq. (1) for the potential at a point i in terms of the six adjacent points j on a rectangular grid is

$$h \sum_{j=1}^6 \epsilon_j (\phi_i - \phi_j) = q_i \quad (3)$$

where ϵ_j is the permittivity at the midpoint between i and j , q_i is the charge assigned to point i , and h is the grid spacing. Placing the grid as in Figure 1(b), yields the set of equations

$$\epsilon_l(\phi_1 - \phi_0) + \epsilon(\phi_1 - \phi_2) = 0 \quad (4)$$

$$\epsilon(\phi_2 - \phi_1) + \epsilon_r(\phi_2 - \phi_3) = 0 \quad (5)$$

where the permittivities, assigned to the midpoints between grid points, are set to ϵ_l if the entire line between the grid points is in the ϵ_l region, and correspondingly for those in the ϵ_r region. Lines between grid points intersecting the boundary, however, have their midpoint permittivity set to some intermediate value ϵ , which will be chosen to make ϕ_1 and ϕ_2 equal the analytic potentials $\phi(1)$ and $\phi(2)$, respectively. Substituting these analytic values from eq. (2) into eq. (4) and solving for ϵ yields

$$\epsilon = \epsilon_l \epsilon_r / (\epsilon_l(1 - a) + \epsilon_r a) \quad (6)$$

The equivalent substitution into eq. (5) yields the same expression.

The identical result is also obtained if the grid is rotated with respect to the axes such that the $x = \text{constant}$ planes are either (110) or (111) planes in the grid and a is taken as the fractional distance along a grid line. Since any surface will approach

local planarity as the grid spacing is decreased, it would appear a reasonable approximation to select ϵ for arbitrary surfaces by letting a be the fractional distance along a grid line at which the surface intersects that line, and then employing eq. (6) to calculate ϵ . This smoothed assignment method, being exact in the limit of small grid spacing, should serve as a better approximation than the current discontinuous assignments in more general geometries.

RESULTS

Electrostatic potential grids have been calculated using both discrete dielectric and smoothed dielectric assignment methods for a point charge q located a distance d from the center of a low dielectric cavity of radius R . This system provides for a simple comparison to an analytic solution. This solution, which can be obtained by the separation of variables, is a series solution in powers of r , and Legendre polynomials of $\cos \theta$. Scaling all of the distances in this model problem (grid spacing, cavity radius, and charge position) will not affect the fractional errors in the potential. All conclusions are thus independent of the particular scale of the problem in question, so the results will be discussed with distances expressed in units of the cavity radius R .

The finite difference calculations were carried out on a 20^3 grid, with the parameters assigned values typical for calculations involving biological molecules. The interior was assigned a dielectric constant of 2 and the exterior a dielectric constant of 78. The grid spacing was chosen to be $R/3$, which is typical of the ratio of the radius of curvature on a biological molecule to the grid spacings necessary to fit a macromolecule on a grid whose density is limited by computer memory and CPU time constraints. Finally, since finite difference methods do not differentiate between point charges and charge distributions smaller than the grid spacing, and do not produce singularities at point charges as expected in the analytic solutions, the charge was located at the center of a box of eight grid points to minimize this deviation and focus attention on the deviations from the continuum solution near the dielectric boundary.

Calculations of the potential using the three methods (analytic, discrete, and smoothed) were carried out for a range of values of d . The finite difference results were compared to series solutions by calculating the absolute value of the fractional difference at each grid point. The maximum error and the RMS of the error for the entire grid are given in Table I, while Figure 2 shows contour plots of the errors in one of the planes of grid points nearest the charge for several of the values of d . As these figures show, the errors are concentrated along the dielectric boundary and are much smaller for the

Table I. Maximum and RMS values for the absolute value of the deviation between analytic and finite difference potentials for a point charge in a low-dielectric cavity of radius R for various distances d of the charge from the center of the cavity, using smoothed or discrete dielectric assignment methods. The calculations were performed on a 20^3 grid with grid spacing $R/3$. Interior and exterior dielectric constants of 2 and 78, respectively, were used.

d/R	Maximum error		RMS error	
	Smoothed	Discrete	Smoothed	Discrete
0.000	0.0996	0.7625	0.0074	0.0562
0.250	0.0973	0.7771	0.0121	0.0564
0.500	0.0963	0.7376	0.0210	0.0501
0.750	0.4088	0.7072	0.0325	0.0580
0.875	0.2129	0.5928	0.0402	0.0505
0.975	3.1317	2.6750	0.1552	0.1171

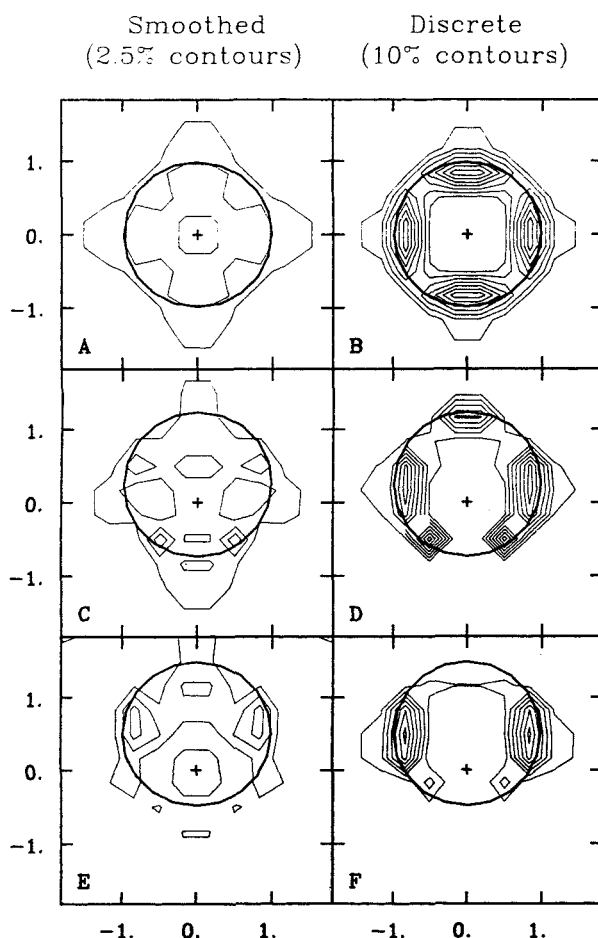


Figure 2. Contour plot of the magnitude of the fractional error for smoothed (a,c,e) and discrete (b,d,f) dielectric assignment methods in the finite difference solution of the electrostatic potential for a point charge in a cavity of radius R with the charge at distances of $0.00R$ (a,b), $0.25R$ (c,d), and $0.50R$ (e,f) from the center of the cavity. Note that the discrete assignment contours are at 10% increments, while the smoothed assignment contours are at 2.5% increments. The charge is always located at the center of the plot, as indicated by the "+" sign. The dark circle indicates the position of the dielectric boundary.

smoothed dielectric than the discrete dielectric. The only exception is the final case where the extremely large errors in both cases arise from the charge spreading beyond the dielectric boundary in the finite difference method. This case will be excluded in practice, since charges are routinely placed at least a van der Waals radius from the boundary. This restriction would in fact preclude the last three cases, keeping the errors in the potential less than 10% for the smoothed dielectric in realistic calculations with a grid spacing of $R/3$.

Figure 3 shows how these methods compare on a protein system, triosephosphate isomerase. The contours represent lines of equal magnitude of the relative difference in the potentials calculated using the two assignment methods. This slice cuts through a surface lysine, Lys67, and is centered near the ζ nitrogen of that residue. For clarity contours interior to the molecule and those for factors larger than two have been omitted. From the figure, it is clear that the smoothed dielectric model yields noticeably different results from the discrete model near this surface lysine.

A more dramatic, and quantifiable demonstration of the smoothed dielectric assignment method's significance can be seen in energy calculations, which are more sensitive to the precise size and shape of the dielectric boundary. Figure 4 shows the results for calculations of solvation energies for spherical

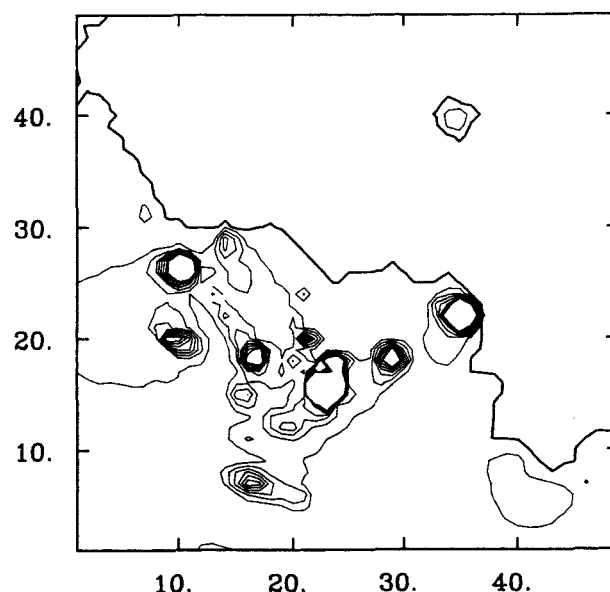


Figure 3. Contour plot of the magnitude of the fractional difference between electrostatic potentials calculated using smoothed and discrete dielectric assignments. This particular view is a cross section of Triosephosphate Isomerase centered near the ζ nitrogen of lysine 67. Values of 2 and 78 were used for the interior and solvent dielectric constants, with a grid spacing of 1.6 \AA . The contours are at 25% increments, but contours interior to the molecule and those greater than a factor of two have been omitted for clarity. The dark line indicates the dielectric boundary.

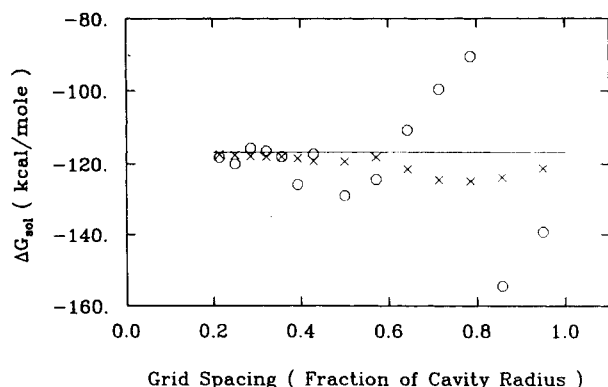


Figure 4. The solvation energy of a spherical, monovalent, 4.0 Å radius ion calculated by a finite difference method as a function of grid spacing for discrete (○) and smooth (×) dielectric assignments. The solid line indicates the analytic value of the energy.

ions, comparing both assignment methods to the analytic result, i.e., the Born solvation energy,⁹

$$\Delta G_{\text{sol}} = \frac{q^2}{4\pi R} \left(\frac{1}{\epsilon} - \frac{1}{\epsilon_0} \right) \quad (7)$$

where q is the charge, ϵ and ϵ_0 are the solvent and vacuum permittivities, and R is the radius of the cavity. Again using a 20^3 grid, the solvation energies were calculated numerically as the difference of the total energy $\frac{1}{2}q\phi$ between a solvent dielectric of 78 and 1. Calculations were made for a range of grid spacings with and without smoothing. The discrete assignments can be seen in the figure to require a much smaller grid spacing to converge to the analytic results. Similarly, Figure 5 shows the improvement to convergence smoothing brings to the calculation of the solvation energy of methanol, modeled as a combination of three spheres of radius 2.1 Å, 1.7 Å, and 1.2 Å for the methyl group, the oxygen, and the hydroxyl hydrogen, respectively.

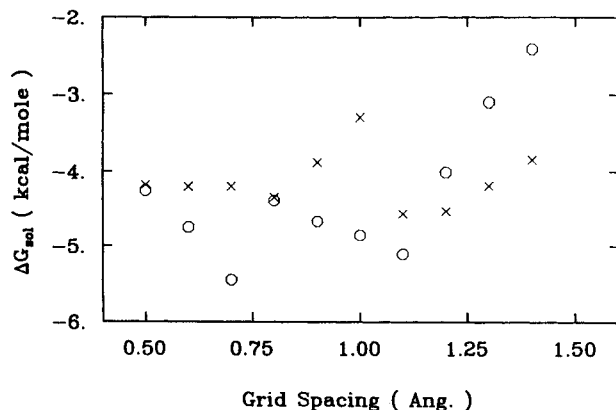


Figure 5. The solvation energy of methanol calculated by a finite difference method as a function of grid spacing for discrete (○) and smooth (×) dielectric assignments.

From these tests, grid spacings of $R/3$ seem quite adequate when smoothing is employed.

Finally, concerning speed of convergence, in all of the test cases and in calculations of the potential around different positions on a 58^3 grid, convergence was obtained in around 5% fewer iterations using the smoothed, as opposed to discrete, dielectric.

DISCUSSION

The application of dielectric smoothing can serve to improve the accuracy of finite difference electrostatic calculations, reducing the maximum errors in the potential at the boundary from around 70% to less than 10% for realistic cases. Electrostatic energy calculations also showed improvement. Convergence to analytic values can be obtained at much larger grid spacings for the smoothed assignments than with the standard discrete methods, permitting accurate calculations on much larger systems. In addition, calculations with model systems as well as larger proteins indicate that the number of iterations required for convergence will be reduced by around 5%. As these three issues are important in finite difference electrostatic calculations, this technique should be of significant value.

This work has been supported in part by NIH, the Robert A. Welch Foundation, ONR, the Texas Advanced Research Program, and the San Diego Supercomputer Center. J.A.M. is the recipient of the George H. Hitchings Award from the Burroughs Wellcome Fund.

References

1. N.K. Rogers, G.R. Moore, and M.J.E. Sternberg, *J. Mol. Biol.*, **182**, 613 (1985).
2. S.H. Northrup, J.O. Boles, and J.C.L. Reynolds, *Science*, **241**, 67 (1988).
3. J.D. Madura and J.A. McCammon, *J. Phys. Chem.*, **93**, 7285 (1989).
4. M.K. Gilson and B. Honig, *Proc. Nat. Acad. Sci.*, **86**, 1524 (1989).
5. J. Warwicker, *J. Mol. Biol.*, **206**, 381 (1989).
6. S. Dao-Pin, D.-I. Liao, and S.J. Remington, *Proc. Nat. Acad. Sci.*, **86**, 5361 (1989).
7. J.J. Sines, S.A. Allison, and J.A. McCammon, *Biochemistry*, **29**, 9403 (1990).
8. D. Bashford and M. Karplus, *Biochemistry*, **29**, 10219 (1990).
9. M.E. Davis and J.A. McCammon, *Chem. Rev.*, **90**, 509 (1990).
10. K.A. Sharp and B. Honig, *Ann. Rev. Biophys. Biophysical Chem.*, **19**, 301 (1990).
11. C.R. Cantor and P.R. Schimmel, *Biophysical Chemistry: Parts I, II, and III*. W.H. Freeman and Company, New York, 1980.
12. I. Klapper, R. Hagstrom, R. Fine, K. Sharp, and B. Honig, *Proteins*, **1**, 47 (1986).
13. D.T. Edmonds, N.K. Rogers, and M.J.E. Sternberg, *Mol. Phys.*, **52**, 1487 (1984).